

This work has been submitted to the IEEE for possible publication. Copyright may be transferred without notice, after which this version may no longer be accessible.

© 2020 IEEE. Personal use of this material is permitted. Permission from IEEE must be obtained for all other uses, in any current or future media, including reprinting/republishing this material for advertising or promotional purposes, creating new collective works, for resale or redistribution to servers or lists, or reuse of any copyrighted component of this work in other works.

Channel Estimation and Equalization for CP-OFDM-based OTFS in Fractional Doppler Channels

Noriyuki HASHIMOTO[†], Noboru OSAWA[†], Kosuke YAMAZAKI[†], and Shinsuke IBI^{††}

[†]KDDI Research, Inc., ^{††}Doshisha University

{ni-hashimoto, nb-oosawa, ko-yamazaki}@kddi-research.jp, sibi@mail.doshisha.ac.jp

Abstract—Orthogonal time frequency and space (OTFS) modulation is a promising technology that satisfies high Doppler requirements for future mobile systems. OTFS modulation encodes information symbols and pilot symbols into the two-dimensional (2D) delay-Doppler (DD) domain. The received symbols suffer from inter-Doppler interference (IDI) in the fading channels with fractional Doppler shifts that are sampled at noninteger indices in the DD domain. IDI has been treated as an unavoidable effect because the fractional Doppler shifts cannot be obtained directly from the received pilot symbols. In this paper, we provide a solution to channel estimation for fractional Doppler channels. The proposed estimation provides new insight into the OTFS input-output relation in the DD domain as a 2D circular convolution with a small approximation. According to the input-output relation, we also provide a low-complexity channel equalization method using the estimated channel information. We demonstrate the error performance of the proposed channel estimation and equalization in several channels by simulations. The simulation results show that in high-mobility environments, the total system utilizing the proposed methods outperforms orthogonal frequency division multiplexing (OFDM) with ideal channel estimation and a conventional channel estimation method using a pseudo sequence.

I. INTRODUCTION

The requirements for future mobile systems are extremely various and strict [1]. For example, the mobility requirement is up to 500 km/h in 5G. Moreover, future mobile systems will require mobility of more than 500 km/h. Future mobile systems are also expected to be launched for nonterrestrial coverages, e.g., underwater, unmanned-aerial-vehicles (UAVs), and low-earth-orbit (LEO) satellites. Due to high Doppler shifts in these environments, orthogonal frequency division multiplexing (OFDM) designed for lower-Doppler environments is no longer effective for these applications.

Orthogonal time frequency and space (OTFS) modulation is a promising technique for addressing this challenge. OTFS was first proposed in [2], [3] where the authors demonstrated that OTFS has outstanding performance compared to the performance of OFDM in high-mobility environments with higher orders of MIMO systems and millimeter-wave systems. Many studies have been performed on OTFS in high-mobility environments [4]–[8] and its application to underwater acoustic channels [9].

In OTFS, all information symbols are mapped onto the two dimensional (2D) delay-Doppler (DD) domain, and the wireless channel is also represented in the DD domain. In [4],

the unavoidable inter-Doppler interference (IDI) is reported to occur in wireless channels composed of multiple paths with the fractional Doppler that cannot be expressed in an integer index in the DD domain. We will refer to these channels as fractional Doppler channels. The message passing (MP) algorithm is also proposed for signal detection to mitigate the IDI in the paper. IDI is unavoidable because the system cannot obtain the fractional Doppler directly. In principle, IDI can be avoided if the fractional Doppler is obtained because the OTFS input-output relation in the DD domain can be expressed as a linear equation. The general channel estimation method for OTFS is to obtain the channel response of the transmitted pilot signals in the DD domain [5]. Using this method, the system can only obtain the channel response indexed to integer numbers in the DD domain. In [7], the pseudo sequence (PN)-based channel estimation method is proposed to estimate the Doppler shift of each path, but the system requires an impractically long PN sequence for accurate estimation of the fractional part.

In this paper, we propose a novel channel estimation method that can handle the fractional Doppler using the pilot response in the DD domain. We also propose a novel low-complexity channel equalization method by using the estimated channel information. Our contributions can be summarized as follows:

- We analyze the IDI caused by the fractional Doppler and the observed channel response of pilot signals in the DD domain. Based on the analysis, we propose a novel cross-correlation-based channel estimation algorithm.
- We formulate an OTFS input-output relation expressed as a 2D circular convolution with a small approximation derived from general channel characteristics. We also propose a novel low-complexity channel equalization method based on this convolutional expression using the proposed channel estimation method.
- Using simulation, we show that the OTFS system using the proposed channel estimation and equalization outperforms OFDM in high-mobility channels by simulations.

Notation: Boldface capital letters represent matrices, and lower-case letters represent column vectors. The transpose, conjugate, conjugate transpose, and inverse of a matrix are denoted by $(\cdot)^T$, $(\cdot)^*$, $(\cdot)^H$, and $(\cdot)^{-1}$, respectively. \otimes is the circular convolution operation. The operator $\text{vec}\{\cdot\}$ denotes the vectorization of a matrix. $(\cdot)_M$ is the modulo operator

of divider M .

II. SYSTEM MODEL

In this section, we first review the basic principle of OTFS proposed in [2]. Then, we explain the CP-OFDM-based OTFS system [8] that we consider in this paper.

A. Basic principle of OTFS

In the OTFS modulation, information symbols (e.g., QAM symbols) are mapped onto the DD domain. The transmitter converts DD domain symbols $X^{\text{DD}}[l, k]$ into the frequency-time (FT) domain symbols $X^{\text{FT}}[m, n]$ using the inverse symplectic finite Fourier transform (ISFFT) as

$$X^{\text{FT}}[m, n] = \frac{1}{\sqrt{MN}} \sum_{k=0}^{N-1} \sum_{l=0}^{M-1} X^{\text{DD}}[l, k] e^{-j2\pi(\frac{ml}{M} - \frac{nk}{N})}. \quad (1)$$

where M and N are the numbers of delay and Doppler bins in the DD domain, respectively.

A time-domain transmit signal $s(t)$ is given by applying the Heisenberg transform to $X^{\text{FT}}[m, n]$ as described by

$$s(t) = \sum_{n=0}^{N-1} \sum_{m=0}^{M-1} X^{\text{FT}}[m, n] e^{j2\pi m \Delta f (t - nT)} g_{\text{tx}}(t - nT) \quad (2)$$

where $g_{\text{tx}}(t)$ is the transmit pulse shape, and T and Δf are the sampling and frequency intervals, respectively, in the FT domain.

The time-domain received signal $r(t)$ in the doubly-selective fading channels is expressed as described by

$$r(t) = \int \int h(\tau, \nu) e^{j2\pi \nu (t - \tau)} s(t - \tau) d\tau d\nu \quad (3)$$

where $h(\tau, \nu)$ is the complex-valued Doppler-variant channel impulse response characterized by delay τ and Doppler frequency ν . Assuming a ray-based quasi-static propagation channel, $h(\tau, \nu)$ is given as

$$h(\tau, \nu) = \sum_{p=1}^P h_p \delta(\tau - \tau_p) \delta(\nu - \nu_p) \quad (4)$$

where P is the number of propagation paths, and $\delta(\cdot)$ denotes the Dirac delta function. Each path is represented by attenuation h_p , delay τ_p , and Doppler frequency ν_p for the p -th path. The delay and Doppler values for the p -th path is given as $\tau_p = \frac{l_{\tau_p}}{M\Delta f}$ and $\nu_p = \frac{k_{\nu_p} + \kappa_{\nu_p}}{NT}$, where l_{τ_p} and k_{ν_p} represent the integer indices of the delay and the Doppler bins in the DD domain, respectively, and κ_{ν_p} is the fractional Doppler that uses a noninteger index to represent ν_p . We consider fractional delays outside the system using the fractional delay filter theory [10].

The receiver performs matched filtering with the receive pulse shape $g_{\text{rx}}(t)$. This operation is known as the cross-ambiguity function $A_{g_{\text{rx}}, r}(\tau, \nu)$ and is given by

$$A_{g_{\text{rx}}, r}(\tau, \nu) \triangleq \int e^{-j2\pi \nu (t - \tau)} g_{\text{rx}}^*(t - \tau) r(t) dt. \quad (5)$$

The FT domain received symbols $Y^{\text{FT}}[m, n]$ is obtained by sampling the cross-ambiguity function $A_{g_{\text{rx}}, r}(\tau, \nu)$ according to

$$Y^{\text{FT}}[m, n] = A_{g_{\text{rx}}, r}(\tau, \nu)|_{\tau=nT, \nu=m\Delta f}. \quad (6)$$

This transformation from the 1D continuous signal $r(t)$ to the 2D symbols $Y^{\text{FT}}[m, n]$ is called the discrete Wigner transform and is the inversion of the Heisenberg transform.

Finally, the receiver performs the symplectic finite Fourier transform (SFFT) to obtain the DD domain received symbols $Y^{\text{DD}}[l, k]$ as described by

$$Y^{\text{DD}}[l, k] = \frac{1}{\sqrt{MN}} \sum_{n=0}^{N-1} \sum_{m=0}^{M-1} Y^{\text{FT}}[m, n] e^{-j2\pi(\frac{nk}{N} - \frac{ml}{M})}. \quad (7)$$

B. Rectangular Pulse Shaping with Cyclic Prefix

To simplify the basic principle of OTFS, let us define the system model in the matrix representations. We consider the OFDM system using the cyclic prefix time guard interval (CP-OFDM) based OTFS system with a single transmit antenna and single receive antenna. The CP-OFDM-based OTFS system is characterized by the rectangular transmit pulse shape that is $1/\sqrt{T}$ for $t \in [0, T)$ and 0 at all other values, and rectangular receive pulse shape, which is $1/\sqrt{T}$ for $t \in [-T_{\text{CP}}, T)$ and 0 at all other values, where T_{CP} is the length of CP.

By introducing the rectangular transmit pulse shape, (2) can be expressed by a symbol-by-symbol block $\mathbf{S} \in \mathbb{C}^{M \times N}$ as

$$\begin{aligned} \mathbf{S} &= \frac{1}{\sqrt{T}} \mathbf{F}_M^H \mathbf{X}^{\text{FT}} \\ &= \frac{1}{\sqrt{T}} \mathbf{X}^{\text{DD}} \mathbf{F}_N^H \end{aligned} \quad (8)$$

where $\mathbf{X}^{\text{FT}} \in \mathbb{C}^{M \times N}$ and $\mathbf{X}^{\text{DD}} \in \mathbb{C}^{M \times N}$ are matrices composed of $X^{\text{FT}}[m, n]$ and $X^{\text{DD}}[l, k]$, respectively, and $\mathbf{F}_M \in \mathbb{C}^{M \times M}$ and $\mathbf{F}_N \in \mathbb{C}^{N \times N}$ are the discrete Fourier transform (DFT) matrices. The CP-OFDM-based OTFS system adds N_{CP} -length CP for each OFDM symbol $\mathbf{s}_i \in \mathbb{C}^M$ that corresponds to $s(t)$ for $(i-1)T \leq t < iT$ in (2) and the column vector of $\mathbf{S} (= [\mathbf{s}_1 \mathbf{s}_2 \dots \mathbf{s}_N])$, to avoid the inter-symbol interference (ISI) among the OFDM symbols via the CP addition matrix $\mathbf{A}_{\text{CP}} \in \mathbb{C}^{(M+N_{\text{CP}}) \times M}$. Finally, the transmitter performs parallel to serial conversions to obtain a transmit signal with CPs $\mathbf{s} \in \mathbb{C}^{(M+N_{\text{CP}})M}$ in the time domain as described by

$$\begin{aligned} \mathbf{s} &= \text{vec}\{\mathbf{A}_{\text{CP}} \mathbf{S}\} \\ &= \frac{1}{\sqrt{T}} \text{vec}\{\mathbf{A}_{\text{CP}} \mathbf{X}^{\text{DD}} \mathbf{F}_N^H\}. \end{aligned} \quad (9)$$

Due to the rectangular pulse shape and avoidance of the ISI with CPs, the i -th received OFDM symbol $\mathbf{r}_i \in \mathbb{C}^M$ after CP removal can be given by

$$\mathbf{r}_i = \mathbf{H}_i \mathbf{s}_i + \mathbf{z}_i \quad (10)$$

where $\mathbf{H}_i \in \mathbb{C}^{M \times M}$ is the channel matrix of the i -th OFDM symbol, and $\mathbf{z}_i \in \mathbb{C}^M$ is the additive noise vector with a zero-mean complex normal distribution with variance σ . Assuming

a ray-based quasi-static propagation channel, \mathbf{H}_i is expressed as

$$\mathbf{H}_i = \sum_{p=1}^P h_p e^{j\phi_p} \Delta_{i,k_{\nu_p},l_{\tau_p}} \mathbf{\Pi}_{l_{\tau_p}} \quad (11)$$

where $\phi_p \in [0, 2\pi)$, $\Delta_{i,k_{\nu_p},l_{\tau_p}} \in \mathbb{C}^{M \times M}$, and $\mathbf{\Pi}_{l_{\tau_p}} \in \mathbb{R}^{M \times M}$ denote the initial phase, the Doppler shift matrix, and the delay matrix, respectively, for the p -th path. The Doppler shift matrix is expressed by $\Delta_{i,k_{\nu_p},l_{\tau_p}} \triangleq \text{diag}[\omega^{(M+N_{\text{CP}})(i-1)+N_{\text{CP}}-l_{\tau_p}}, \omega^{(M+N_{\text{CP}})(i-1)+N_{\text{CP}}-l_{\tau_p}+1}, \dots, \omega^{(M+N_{\text{CP}})(i-1)+N_{\text{CP}}-l_{\tau_p}+M-1}]$ where $\omega = e^{\frac{j2\pi(k_{\nu_p}+\kappa_{\nu_p})}{(M+N_{\text{CP}})N}}$. The delay matrix $\mathbf{\Pi}_{l_{\tau_p}}$ is the forward cyclic shifted permutation matrix according to delay l_{τ_p} in the DD domain.

The receiver performs M -point DFT on the i -th OFDM symbol in the time domain to obtain the frequency domain symbol vector $\mathbf{y}_i^{\text{FT}} \in \mathbb{C}^{M \times 1}$ as

$$\begin{aligned} \mathbf{y}_i^{\text{FT}} &= \mathbf{F}_M \mathbf{r}_i \\ &= \mathbf{F}_M (\mathbf{H}_i \mathbf{s}_i + \mathbf{z}_i) \\ &= \mathbf{F}_M \mathbf{H}_i \mathbf{X}^{\text{DD}} \mathbf{f}_i^* + \mathbf{F}_M \mathbf{z}_i \end{aligned} \quad (12)$$

where $\mathbf{f}_i \in \mathbb{C}^N$ is the i -th column vector of \mathbf{F}_N . Let $\mathbf{Y}^{\text{FT}} \triangleq [\mathbf{y}_1^{\text{FT}}, \mathbf{y}_2^{\text{FT}}, \dots, \mathbf{y}_N^{\text{FT}}] \in \mathbb{C}^{M \times N}$ denote the 2D received symbols in the FT domain. Applying the SFFT to \mathbf{Y}^{FT} , we obtain the DD domain symbol matrix $\mathbf{Y}^{\text{DD}} \in \mathbb{C}^{M \times N}$ as

$$\begin{aligned} \mathbf{Y}^{\text{DD}} &= \mathbf{F}_M^H \mathbf{Y}^{\text{FT}} \mathbf{F}_N \\ &= \sum_{i=1}^N \mathbf{F}_M^H \mathbf{y}_i^{\text{FT}} \mathbf{f}_i^T \\ &= \sum_{i=1}^N \mathbf{H}_i \mathbf{X}^{\text{DD}} \mathbf{f}_i^* \mathbf{f}_i^T + \mathbf{z}_i \mathbf{f}_i^T. \end{aligned} \quad (13)$$

Based on (11) and (13), each element $Y^{\text{DD}}[l, k]$ of \mathbf{Y}^{DD} without the noise term can be expressed as

$$\begin{aligned} Y^{\text{DD}}[l, k] &= \sum_{i=1}^N \sum_{l'=0}^{M-1} \sum_{k'=0}^{N-1} \left[\sum_{p=1}^P h_p \delta((l-l')_M - l_{\tau_p}) e^{j\phi_p} \right. \\ &\quad \cdot e^{j2\pi(k_{\nu_p}+\kappa_{\nu_p}) \frac{(M+N_{\text{CP}})(i-1)+N_{\text{CP}}-l_{\tau_p}+l}{(M+N_{\text{CP}})N}} \\ &\quad \cdot X^{\text{DD}}[l', k'] e^{-j2\pi \frac{(i-1)(k-k')}{N}} \\ &= \sum_{l'=0}^{M-1} \sum_{k'=0}^{N-1} X^{\text{DD}}[l', k'] \Lambda_l[(l-l')_M, (k-k')_N]. \end{aligned} \quad (14)$$

$$\begin{aligned} \because \Lambda_l[(l-l')_M, (k-k')_N] &\triangleq \sum_{p=1}^P h_p \delta((l-l')_M - l_{\tau_p}) \\ &\quad \cdot \Upsilon_N((k_{\nu_p} + \kappa_{\nu_p} - (k-k'))_N) \\ &\quad \cdot e^{j\phi_p} \psi_p[l] \end{aligned}$$

$$\because \Upsilon_N(x) \triangleq \sum_{i=1}^N e^{j2\pi(i-1)\frac{x}{N}} = \frac{\sin(\pi x)}{\sin(\pi \frac{x}{N})} e^{j\pi \frac{x(N-1)}{N}}$$

$$\because \psi_p[l] \triangleq e^{j2\pi(k_{\nu_p}+\kappa_{\nu_p}) \frac{N_{\text{CP}}-l_{\tau_p}+l}{(M+N_{\text{CP}})N}}$$

The vectorized version of \mathbf{Y}^{DD} can be represented as

$$\begin{aligned} \mathbf{y}^{\text{DD}} &= \text{vec}\{\mathbf{Y}^{\text{DD}}\} \\ &= (\mathbf{F}_N \otimes \mathbf{I}_M) \mathbf{H} (\mathbf{F}_N^H \otimes \mathbf{I}_M) \mathbf{x}^{\text{DD}} + (\mathbf{F}_N \otimes \mathbf{I}_M) \mathbf{z} \\ &= \Phi \mathbf{x}^{\text{DD}} + (\mathbf{F}_N \otimes \mathbf{I}_M) \mathbf{z} \end{aligned} \quad (15)$$

where $\mathbf{H} = \text{diag}[\mathbf{H}_1, \mathbf{H}_2, \dots, \mathbf{H}_N]$, $\mathbf{x}^{\text{DD}} = \text{vec}\{\mathbf{X}^{\text{DD}}\}$, $\mathbf{z} = [\mathbf{z}_1^T, \mathbf{z}_2^T, \dots, \mathbf{z}_N^T]^T$, and $\Phi = (\mathbf{F}_N \otimes \mathbf{I}_M) \mathbf{H} (\mathbf{F}_N^H \otimes \mathbf{I}_M)$.

III. FRACTIONAL DOPPLER ANALYSIS

Equation (14) indicates that the received symbols $Y^{\text{DD}}[l, k]$ are affected by the fractional Doppler through $\Upsilon_N((k_{\nu_p} + \kappa_{\nu_p} - (k-k'))_N)$. Considering $\Upsilon_N(k + \kappa)$, $k \in \mathbb{Z}$, $\kappa \in [0, 1)$, $\Upsilon_N(k + \kappa)$ is localized at k only in the absence of fractional Doppler ($\kappa = 0$). By contrast, nonzero values of $0 < |\Upsilon_N(k + \kappa)| < N$ appear according to κ at any k when $\kappa \neq 0$. Thus, this is the source of the IDI.

Let us consider the channel response $\tilde{H}_{i,j}^{\text{DD}}[l, k]$ of a pilot signal $X_{i,j}^{\text{DD}}[l, k]$ in the DD domain

$$X_{i,j}^{\text{DD}}[l, k] = \begin{cases} 1 & \text{if } l = i, k = j \\ 0 & \text{otherwise} \end{cases}. \quad (16)$$

From (14), the channel response of the pilot signal can be written as

$$\begin{aligned} \tilde{H}_{i,j}^{\text{DD}}[l, k] &= \sum_{p=1}^P e^{j\phi_p} \psi_p[l] h_p \delta((l-i)_M - l_{\tau_p}) \\ &\quad \cdot \Upsilon_N((k_{\nu_p} + \kappa_{\nu_p} - (k-j))_N). \end{aligned} \quad (17)$$

The pilot signal is observed from the above equation as multiple paths with an integer Doppler shift that is different from the actual Doppler shift in the Doppler domain over the fractional Doppler channels. Since the observed Doppler shifts are different from the actual Doppler shift, the direct use of the information from (17) for signal detection results in detection error unless the inversion operation in (14) is performed.

IV. CHANNEL ESTIMATION

In this section, we propose a channel estimation method using the cross-correlation of $\tilde{H}_{i,j}^{\text{DD}}[l, k]$ with $\Upsilon_N(k + \kappa)$ across Doppler domain elements. The normalized cross-correlation function for all k between $\tilde{H}_{i,j}^{\text{DD}}[l, k]$ on the l -th delay bin and $\Upsilon_N(k + \kappa)$ with parameter κ corresponding to the fractional Doppler is given by

$$R_{H_l, \Upsilon}(k + \kappa) = \frac{1}{N^2} \sum_{k'=0}^{N-1} \tilde{H}_{i,j}^{\text{DD}}[l, k'] \Upsilon_N^*((k' - (k + \kappa))_N). \quad (18)$$

For simplicity, let us consider a channel having a single path on the l -th delay bin and the pilot signal in the DD domain of $i = j = 0$. When the estimated Doppler index $k + \kappa$ matches the actual Doppler index $k_{\nu_p} + \kappa_{\nu_p}$ of the p -th path, this function reaches the highest magnitude, i.e., $|R_{H_l, \Upsilon}(k + \kappa)| = h_p$. Therefore, by finding the highest magnitude of the function with $k + \kappa$, we can completely

Algorithm 1 Proposed Channel Estimation

Input: Pilot response matrix $\tilde{H}_{i,j}^{\text{DD}}$, thresholds α and β , and noise variance σ_n^2
Initialize $\hat{p} \leftarrow 1$
for each delay l **do**
 Initialize $H' \leftarrow \tilde{H}_{i,j}^{\text{DD}}[l, :]$
 repeat
 Find $k + \kappa$ with the maximum value of $|R_{H', \Upsilon}(k + \kappa)|$ using H'
 Estimate $\hat{\kappa}_{\nu_{\hat{p}}} + \hat{\kappa}_{\nu_{\hat{p}}}$, $\hat{l}_{\tau_{\hat{p}}}$, $\hat{h}_{\hat{p}}$, $\hat{\psi}_{\hat{p}}$, and $\hat{\phi}_{\hat{p}}$
 Update $H' \leftarrow H' - \hat{h}_{\hat{p}} e^{j\hat{\phi}_{\hat{p}}} \hat{\psi}_{\hat{p}}[\hat{l}_{\tau_{\hat{p}}}] \Upsilon_N(\hat{\kappa}_{\nu_{\hat{p}}} + \hat{\kappa}_{\nu_{\hat{p}}})$.
 Update $\hat{p} \leftarrow \hat{p} + 1$
 until Stopping criteria of (20)
end for
Output: Path parameters $\hat{\kappa}_{\nu_{\hat{p}}} + \hat{\kappa}_{\nu_{\hat{p}}}$, $\hat{l}_{\tau_{\hat{p}}}$, $\hat{h}_{\hat{p}}$, and $\hat{\phi}_{\hat{p}}$ for all \hat{p}

estimate the channel parameters for the l -th delay bin as follows:

$$\left\{ \begin{array}{l} \hat{\kappa}_{\nu_{\hat{p}}} + \hat{\kappa}_{\nu_{\hat{p}}} = k + \kappa, \\ \hat{l}_{\tau_{\hat{p}}} = l, \\ \hat{h}_{\hat{p}} = |R_{H', \Upsilon}(\hat{\kappa}_{\nu_{\hat{p}}} + \hat{\kappa}_{\nu_{\hat{p}}})|, \\ \hat{\psi}_{\hat{p}} = e^{j2\pi(\hat{\kappa}_{\nu_{\hat{p}}} + \hat{\kappa}_{\nu_{\hat{p}}}) \frac{N_{\text{CP}} - \hat{l}_{\tau_{\hat{p}}}}{(M + N_{\text{CP}})N}}, \\ e^{j\hat{\phi}_{\hat{p}}} = \frac{R_{H', \Upsilon}(\hat{\kappa}_{\nu_{\hat{p}}} + \hat{\kappa}_{\nu_{\hat{p}}})}{|R_{H', \Upsilon}(\hat{\kappa}_{\nu_{\hat{p}}} + \hat{\kappa}_{\nu_{\hat{p}}})|} \hat{\psi}_{\hat{p}}^{-1}. \end{array} \right. \quad (19)$$

For multipath scenarios, the estimated path based on (19) is removed from the pilot response $\tilde{H}_{i,j}^{\text{DD}}$, and then the estimation is iteratively executed as described in Algorithm 1. The estimation algorithm stops when the maximum value of $|R_{H', \Upsilon}(k + \kappa)|$ for all $k + \kappa$ satisfies at least one of the following criteria:

$$\max |R_{H', \Upsilon}(k + \kappa)| < \begin{cases} \alpha \left| \sum_{i=1}^N \tilde{H}_{i,j}^{\text{DD}}[l, i] \right| \\ \beta \sigma. \end{cases} \quad (20)$$

where α and β are tuning coefficients.

V. CHANNEL EQUALIZATION

Based on (14), $\Lambda_l[(l - l')_M, (k - k')_N]$ can be regarded as an effective channel in the DD domain, but it represents different channels according to the delay index l because of the Doppler shift $\psi_p[l]$. If $\psi_p[l]$ is constant (e.g., no Doppler shift) at any l , the received symbol matrix can be expressed as $\mathbf{Y}^{\text{DD}} = \mathbf{X}^{\text{DD}} \otimes \Lambda_l$, where $\Lambda_l \in \mathbb{C}^{M \times N}$ is the matrix composed of $\Lambda_l[l, k]$ for $l = 0, \dots, M-1, k = 0, \dots, N-1$. Even if $\psi_p[l]$ is not constant, we can observe that differences in $\psi_p[l]$ between a delay bin l and adjacent delay bins are negligibly small. This is because the differences depend on the Doppler index $\kappa_{\nu_p} + \kappa_{\nu_p}$ and the frame length $(M + N_{\text{CP}})N$ from (14), but the frame length is dominant (i.e., $\frac{\kappa_{\nu_p} + \kappa_{\nu_p}}{(M + N_{\text{CP}})N} \ll 1$).

In addition, $\mathbf{Y}^{\text{DD}}[l, k]$ is composed of $X^{\text{DD}}[l', k']$ and $\Lambda_l[(l - l')_M, (k - k')_N]$ with an index l' that can only be a close value

to the index l in practice because the channel impulse response $h(\tau, \nu)$ is usually localized (i.e., $l_{\tau_p} \ll M$) in the delay domain i.e., $\Lambda_l[(l - l')_M, (k - k')_N] = 0$ if $(l - l')_M - l_{\tau_p} > 0$. These observations indicate that the l -th symbols of \mathbf{Y}^{DD} can be represented by the 2D circular convolution of \mathbf{X}^{DD} and Λ'_l , which is a matrix generated from the constant phase shift $\psi_{p,l}$ defined by the delay index l of $\mathbf{Y}^{\text{DD}}[l, k]$ instead of $\psi_p[l]$ in (14), as

$$\mathbf{Y}^{\text{DD}}[l, k] \approx (\mathbf{X}^{\text{DD}} \otimes \Lambda'_l)[l, k]. \quad (21)$$

Since Λ'_l can be derived from the estimated path parameters described in the previous section, we can obtain the estimated transmit symbols on delay bin l by applying the 2D Wiener deconvolution [11] as

$$\mathcal{F}(\hat{\mathbf{X}}_l^{\text{DD}})[\eta, \xi] = \frac{\mathcal{F}(\Lambda'_l)^*[\eta, \xi]}{|\mathcal{F}(\Lambda'_l)[\eta, \xi]|^2 + \sigma_n^2} \mathcal{F}(\mathbf{Y}^{\text{DD}})[\eta, \xi], \quad (22)$$

$$\hat{X}^{\text{DD}}[l, k] = \mathcal{F}^{-1}(\mathcal{F}(\hat{\mathbf{X}}_l^{\text{DD}}))[l, k], \quad (23)$$

where $\mathcal{F}(\cdot)$ denotes the 2D DFT, $\xi = 0, \dots, N-1$, and $\eta = 0, \dots, M-1$.

The dominant computational complexity of this operation arises from the 2D DFT and 2D IDFT. When M and N are numbers equal to powers of two, the complexity of 2D DFT and 2D IDFT is $O(MN \log MN)$ due to the use of the fast Fourier transform (FFT) algorithm. Since this operation requires at most M iterations to obtain $\hat{\mathbf{X}}_l^{\text{DD}}$ for all delays, the total computational complexity is $O(M^2 N \log MN)$. By contrast, the equalization based on the matrix inversion of (15) has $O(M^3 N^3)$ complexity.

Note: This method requires high channel estimation accuracy, according to the signal-to-noise ratio (SNR). The denominator of (22) can be close to zero. If the channel estimation error causes the error, the error is enhanced by the division, and then the error is spread to many elements by operation (23). When this error degrades the performance, the magnitude of $|\mathcal{F}(\Lambda'_l)[\eta, \xi]|^2$ in (22) should be modified locally to avoid division by zero or values close to zero [12].

VI. SIMULATION RESULTS

This section presents the bit error performance of the OTFS system with the proposed channel estimation and equalization under different parameters and environments. Table I provides relevant parameters for all simulations. For each channel, fractional delay filters using Farrow structures [10] are used to implement the fractional delay. Each of the Doppler shift is given by Jakes' formula as

$$\nu_p = \nu_{\max} \cos(\theta_p) \quad (24)$$

where ν_{\max} is the maximum Doppler shift determined by the user speed and angle-of-arrival θ_p that is uniformly distributed over $[-\pi, \pi)$. To evaluate the channel estimation method, we consider the PN-sequence-based estimation [7] using two different lengths of the pilot sequence. The first sequence is the same length as the information, and the second sequence is ten times longer because this method requires a long sequence for

TABLE I
SIMULATION PARAMETERS

Parameter	Value
Carrier frequency	4.5 GHz
# of subcarriers (M)	256
# of OFDM symbols (N)	14
Subcarrier spacing (Δf)	15 kHz
CP length (N_{CP})	17 samples (6.67% of M)
Channel profile	MED [13] with max. delay of the CP length and TDL-C [14] with 300 ns RMS delay
User speed	500 km/h for MED, 120 km/h for TDL-C

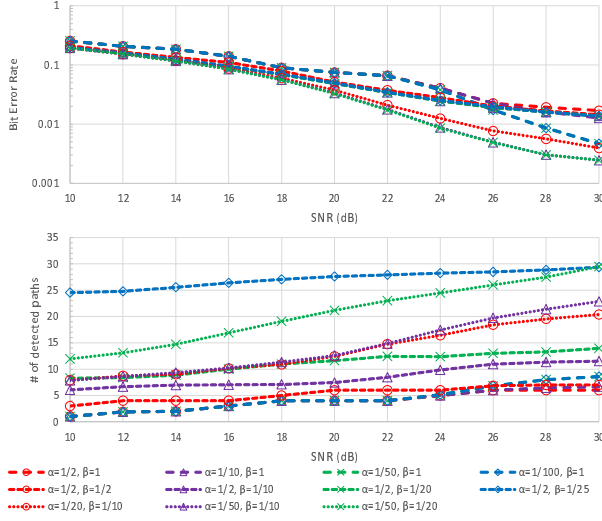


Fig. 1. Bit error rate (BER) of 64-QAM (top) and the number of paths detected by the proposed estimation method (bottom) with different values of α and β in (20) in the MED channel with 10 paths and a speed of 500 km/h.

precise estimation of Doppler frequencies. In all simulations, the pilot signals are ideally distorted by the same channel with the information signal and the complex Gaussian noise of the same level as the information signal. This is a simplification for the simulation, but the impact on the performance is small even if the pilot and information are sent at different frames (e.g., the adjacent frames) because the OTFS signal is modulated in the DD domain and the channel represented in the DD domain does not vary considerably over the period.

We first study the coefficients α and β of the stopping criteria in (20) since the performance and the number of iterations of Algorithm 1 depend on these coefficients. Fig. 1 shows the BER performance and the number of detected paths with different values of the coefficients. Better error performance and fewer detected paths indicate the best choice for the coefficients. Based on the results, we choose $\alpha = 1/50$ and $\beta = 1/10$ for the subsequent simulations.

Next, we show comparisons of the channel estimation methods between the proposed method and the use of the pilot response of (17) directly, and comparisons of the equalization methods between the proposed method, the Wiener deconvolution without the proposed approximation, and the matrix inversion of (15) in Fig. 2. First, this result indicates

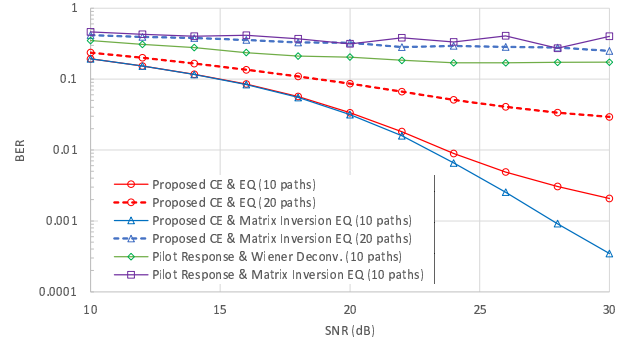


Fig. 2. Performance comparisons of the proposed channel estimation, the equalization to the direct use of the pilot response, and the matrix inversion equalizer in the MED channels with 10 and 20 paths and a speed of 500 km/h.

that the direct use of the pilot response as an estimated channel does not equalize the signal in the fractional Doppler channel. In the MED with 10 paths, the matrix inversion equalization is slightly better than the proposed method in the high SNR region because of the approximation in the proposed equalization. By contrast, the result is opposite for the channel with 20 paths. In the MED channel, each path is placed at equal intervals in the delay domain. The proposed channel estimation can almost correctly estimate the MED channel with 10 paths because there is almost a single path in a delay bin in this simulation settings. By contrast, the channel estimation accuracy decreases in the MED channel with 20 paths because there are several paths in the same delay bin. This means that the proposed equalization method is robust against the channel estimation error.

Third, we compare the proposed channel estimation with the PN-sequence-based channel estimation in the MED channels. An examination of the results presented in Fig. 3 shows that the proposed method outperforms the PN-sequence-based channel estimation regardless of the channels even when the long PN sequence is used. By contrast, as noted in Section V, channel estimation errors degrade the performance because of the low estimation accuracy with a short sequence.

Finally, Fig. 4 shows uncoded and coded bit error performances in the TDL-C channel with a mobile speed of 120 km/h in order to compare OTFS and OFDM. We adopt the Turbo coding with 1/2 coding rate and 8 iterations for the decoder in this simulation to validate the effectiveness of the error correction coding for the proposed method. The TDL-C channel has 24 paths and most of the paths are located close to the first path. Although for the proposed method, estimation of the TDL-C channel is more challenging due to this path characteristic than the estimation of the MED channel, the proposed method provides a better performance than OFDM that uses the frequency domain minimum mean square error (MMSE) equalizer with an ideal symbol-by-symbol channel impulse response. Compared to uncoded and coded performances, the error correction coding is more effective for OTFS than for OFDM. This indicates that the OTFS error distribution

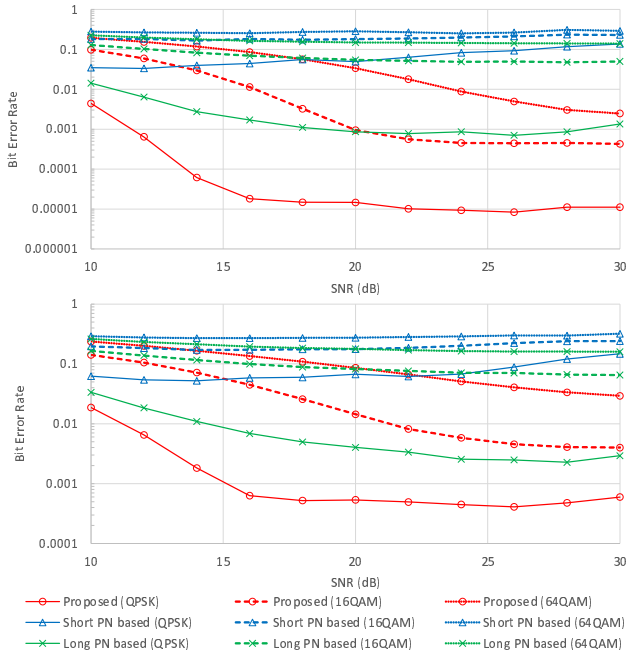


Fig. 3. Comparisons of BER performance characteristics of the proposed channel estimation and the conventional PN-sequence-based channel estimation with two different sequence lengths in the MED channel with 10 (top) and 20 (bottom) paths and a speed of 500 km/h.

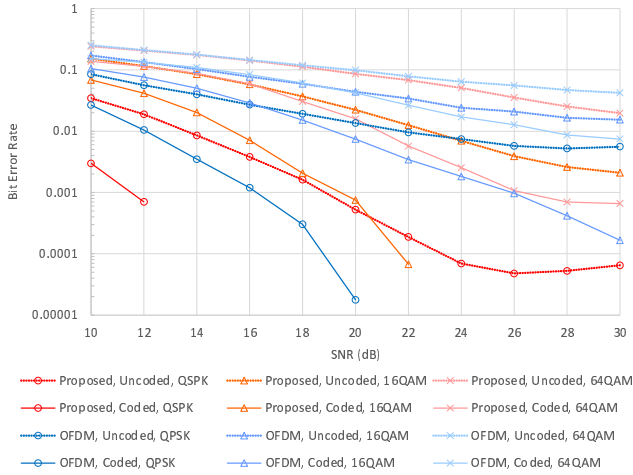


Fig. 4. Comparison of uncoded and coded bit error performances between OTFS using the proposed methods and MMSE-OFDM in the TDL-C channel with a speed of 120 km/h. The Turbo coding with 1/2 coding rate and decoding with 8 iterations is used.

fits the Gaussian distribution well. In addition, as described in the first part of this section, we assume the information and pilot signals through the same channel in this simulation. This assumption does not have a significant effect for OTFS, but it degrades the performance of OFDM from the current result in a real situation where the information and pilot are sent at different times because the channel represented in the frequency domain varies rapidly with time in high-mobility environments.

VII. CONCLUSION

We analyzed the effect of the fractional Doppler in the delay-Doppler domain for OTFS. This analysis allowed the construction of a novel channel estimation method using the pilot response in the delay-Doppler domain. Based on the estimation, we also proposed a novel low-complexity equalizer.

Simulation results show that the proposed estimation method displays a more reliable channel estimation accuracy than the conventional PN-sequence-based channel estimation in several channels. The total system with the proposed channel estimation and equalization outperforms OFDM in high-mobility environments without the use of any iterative signal detection methods.

Topics for future work include iterative signal detection approaches with small numbers of iterations for improving the performance with practical complexity. The proposed channel estimation method will also help remedy the complexity of joint radar and communication applications using OTFS due to the high channel estimation accuracy.

REFERENCES

- [1] N. Rajatheva *et al.*, “White Paper on Broadband Connectivity in 6G,” *arXiv:2004.14247 [eess]*, Apr. 2020. arXiv: 2004.14247.
- [2] R. Hadani, S. Rakib, M. Tsatsanis, A. Monk, A. J. Goldsmith, A. F. Molisch, and R. Calderbank, “Orthogonal Time Frequency Space Modulation,” in *2017 IEEE Wireless Communications and Networking Conference (WCNC)*, pp. 1–6, Mar. 2017.
- [3] R. Hadani, S. Rakib, A. F. Molisch, C. Ibars, A. Monk, M. Tsatsanis, J. Delfeld, A. Goldsmith, and R. Calderbank, “Orthogonal Time Frequency Space (OTFS) modulation for millimeter-wave communications systems,” in *2017 IEEE MTT-S International Microwave Symposium (IMS)*, pp. 681–683, June 2017.
- [4] P. Raviteja, K. T. Phan, Y. Hong, and E. Viterbo, “Interference Cancellation and Iterative Detection for Orthogonal Time Frequency Space Modulation,” *IEEE Transactions on Wireless Communications*, vol. 17, pp. 6501–6515, Oct. 2018.
- [5] M. Kollengode Ramachandran and A. Chockalingam, “MIMO-OTFS in High-Doppler Fading Channels: Signal Detection and Channel Estimation,” in *2018 IEEE Global Communications Conference (GLOBECOM)*, pp. 206–212, IEEE, Dec. 2018.
- [6] P. Raviteja, K. T. Phan, and Y. Hong, “Embedded Pilot-Aided Channel Estimation for OTFS in Delay-Doppler Channels,” *IEEE Transactions on Vehicular Technology*, vol. 68, pp. 4906–4917, May 2019.
- [7] K. R. Murali and A. Chockalingam, “On OTFS Modulation for High-Doppler Fading Channels,” in *2018 Information Theory and Applications Workshop (ITA)*, pp. 1–10, IEEE, Feb. 2018.
- [8] W. Shen, L. Dai, J. An, P. Fan, and R. W. Heath, “Channel Estimation for Orthogonal Time Frequency Space (OTFS) Massive MIMO,” *IEEE Transactions on Signal Processing*, vol. 67, pp. 4204–4217, Aug. 2019.
- [9] M. J. Bocus, A. Doufexi, and D. Agrafiotis, “Performance of OFDM-based massive MIMO OTFS systems for underwater acoustic communication,” *IET Communications*, vol. 14, pp. 588–593, Mar. 2020.
- [10] V. Välimäki and T. I. Laakso, *Fractional Delay Filters—Design and Applications*. Boston, MA: Springer US, 2001.
- [11] G. Dougherty and Z. Kawaf, “The point spread function revisited: Image restoration using 2-D deconvolution,” *Radiography*, vol. 7, pp. 255–262, Nov. 2001.
- [12] I. Pitas, *Digital Image Processing Algorithms and Applications*. USA: John Wiley & Sons, Inc., 1st ed., 2000.
- [13] M. Patzold, A. Szczepanski, and N. Youssef, “Methods for modeling of specified and measured multipath power-delay profiles,” *IEEE Transactions on Vehicular Technology*, vol. 51, pp. 978–988, Sept. 2002. Conference Name: IEEE Transactions on Vehicular Technology.
- [14] *3GPP TR38.901: Study on channel model for frequencies from 0.5 to 100 GHz*. 3rd Generation Partnership Project (3GPP), Mar. 2017. Release 14.

APPENDIX

PROOF OF (14): OTFS INPUT-OUTPUT RELATION IN THE DELAY-DOPPLER DOMAIN

We start with defining elements of each matrix composed of (14). By using the Dirac delta function, each element of the delay matrix $\Pi_{l_{\tau_p}}$ can be written as

$$\Pi_{l_{\tau_p}}[l, l'] = \delta((l - l')_M - l_{\tau_p}). \quad (25)$$

Therefore, each element of \mathbf{H}_i can be expressed as

$$H_i[l, l'] = \sum_{p=1}^P h_p e^{j\phi_p} \delta((l - l')_M - l_{\tau_p}) \cdot e^{j2\pi(k_{\nu_p} + \kappa_{\nu_p}) \frac{(M+N_{\text{CP}})(i-1) + N_{\text{CP}} - l_{\tau_p} + l}{(M+N_{\text{CP}})N}} \quad (26)$$

The signal part of (13) can be written as

$$\sum_{i=1}^N \mathbf{H}_i \mathbf{X}^{\text{DD}} \mathbf{f}_i^* \mathbf{f}_i^T = \sum_{i=1}^N \mathbf{H}_i \mathbf{X}^{\text{DD}} \boldsymbol{\Omega}_i \quad (27)$$

$$\because \Omega_i[k, k'] = e^{-j2\pi \frac{(i-1)(k-k')}{N}}$$

Based on (26) and (27), $Y^{\text{DD}}[l, k]$ can be obtained as shown in (28), which completes the proof.

$$\begin{aligned} Y^{\text{DD}}[l, k] &= \sum_{i=1}^N \sum_{l'=0}^{M-1} \sum_{k'=0}^{N-1} H_i[l, l'] X^{\text{DD}}[l', k'] \Omega_i[k', k] \\ &= \sum_{i=1}^N \sum_{l'=0}^{M-1} \sum_{k'=0}^{N-1} \left[\sum_{p=1}^P h_p \delta((l - l')_M - l_{\tau_p}) e^{j\phi_p} e^{j2\pi(k_{\nu_p} + \kappa_{\nu_p}) \frac{(M+N_{\text{CP}})(i-1) + N_{\text{CP}} - l_{\tau_p} + l}{(M+N_{\text{CP}})N}} \right] X^{\text{DD}}[l', k'] e^{-j2\pi \frac{(i-1)(k-k')}{N}} \\ &= \sum_{l'=0}^{M-1} \sum_{k'=0}^{N-1} X^{\text{DD}}[l', k'] \sum_{p=1}^P h_p \delta((l - l')_M - l_{\tau_p}) e^{j\phi_p} \sum_{i=1}^N e^{j2\pi(k_{\nu_p} + \kappa_{\nu_p}) \frac{(M+N_{\text{CP}})(i-1) + N_{\text{CP}} - l_{\tau_p} + l}{(M+N_{\text{CP}})N}} e^{-j2\pi \frac{(i-1)(k-k')}{N}} \\ &= \sum_{l'=0}^{M-1} \sum_{k'=0}^{N-1} X^{\text{DD}}[l', k'] \sum_{p=1}^P h_p \delta((l - l')_M - l_{\tau_p}) e^{j\phi_p} e^{j2\pi(k_{\nu_p} + \kappa_{\nu_p}) \frac{N_{\text{CP}} - l_{\tau_p} + l}{(M+N_{\text{CP}})N}} \sum_{i=1}^N e^{j2\pi(k_{\nu_p} + \kappa_{\nu_p}) \frac{i-1}{N}} e^{-j2\pi \frac{(i-1)(k-k')}{N}} \\ &= \sum_{l'=0}^{M-1} \sum_{k'=0}^{N-1} X^{\text{DD}}[l', k'] \sum_{p=1}^P h_p \delta((l - l')_M - l_{\tau_p}) e^{j\phi_p} e^{j2\pi(k_{\nu_p} + \kappa_{\nu_p}) \frac{N_{\text{CP}} - l_{\tau_p} + l}{(M+N_{\text{CP}})N}} \sum_{i=1}^N e^{j2\pi(i-1) \frac{(k_{\nu_p} + \kappa_{\nu_p}) - (k-k')}{N}} \\ &= \sum_{l'=0}^{M-1} \sum_{k'=0}^{N-1} X^{\text{DD}}[l', k'] \Lambda_l[(l - l')_M, (k - k')_N] \end{aligned} \quad (28)$$